ATLAS Internal Note

Characterization of the new 8-stages Hamamatsu photomultipliers for the July 98 Test Beam

M. Crouau, P. Grenier, C. Hebrard, G. Montarou

Laboratoire de Physique Corpusculaire
Université Blaise Pascal/CNRS-IN2P3
63177 AUBIERE CEDEX

F. Camarena

Departamento de física Atómica, Molecular y Nuclear
Univ. of VALENCIA and IFIC
Centro Mixto Univ. of Valencia - CSIC
Avda. Dr. Moliner 50, E-46100 Burjassot
VALENCIA, Spain

Introduction:

This note presents the characterization of the 52 new R5900 8 stages Hamamatsu photomultipliers which have been used during the 1998 Tilecal test beam. The PMTs have been measured in the test bench prototype [1] using a procedure very close to the one foreseen for the characterization of the ten thousand PMTs for ATLAS. Special dividers have been used for the quantum efficiency, amplification in DC mode and relative photocathode sensitivity measurements. Standard dividers have been used for the amplification in pulsed mode, dark current and linearity measurements.

1.Quantum Efficiency

For the July 98 test beam 52 new R5900 8 stages PMTs have been used, with new making process and new photocathode window material. These modifications are lead to an improvement of the quantum efficiency compared to the previous generations of PMTs. An increase from 16% to 18.5% will be shown from the results of our measurements.

We have done the Q.E. measurement for all the PMTs in the test bench prototype. The procedure consists in measuring, using a slow ADC, the current generated by the PMT operated in photocathode mode and to compare it with the current registered by a photodiode for the same quantity of light. A large area (18x18 mm^2) Hamamatsu photodiode (ref. S3204-04) was used. This photodiode was previously calibrated at several wavelengths by Hamamatsu. At 480nm, the Q.E. was estimated to be 70.1%. In order to equalize the light we had to intercalibrate each light channel; it was done by moving the PMTs from their channel to the reference point. In order to get the photocathode mode we used the special dividers which have relays that allow to select between the anode and photocathode mode.

In this case the Q.E. is proportional to the current, so we have the relation:

$$QE_{PMT} = QE_{PD} \times \frac{I_{PMT} \times C_i}{I_{PD}} \tag{1}$$

where C_i are the calibration coefficients between the PMT channels and the photodiode channel, and I_{PMT} and I_{PD} are the current registered in the photomultiplier and photodiode respectivily. The results of the calibration are given in table 1. Figure 1 shows the position of all the elements used for the measurement.

CHANNEL	C_i Coefficients
0	1.175 ± 0.012
1	1.169 ± 0.012
2	1.146 ± 0.011
3	1.021 ± 0.010
4	1.038 ± 0.010

Table 1: *Light calibration reference-channel coefficients.*

The repeatibility of the calibration shows a variation of calibration factors less than 1%. Doing the calibration with another set of PMTs the variation in the calibration coefficients are less than 2%. So we can conclude that our quantum efficiency measurement are done with an accuracy of around 2%. Figure 2 shows the Hamamatsu results together with our results. Figure 3 represents the correlation between them.

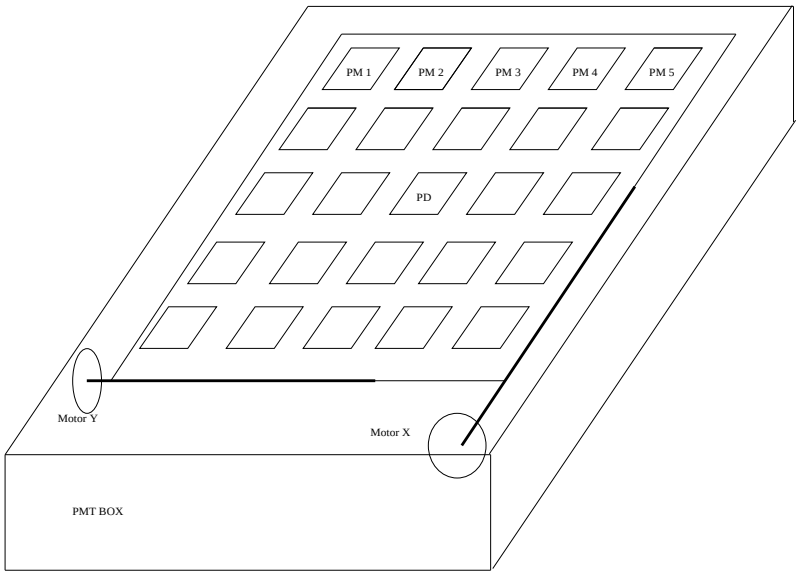

Figure 1: *Setup used for the measurement of the quantum efficiency.*

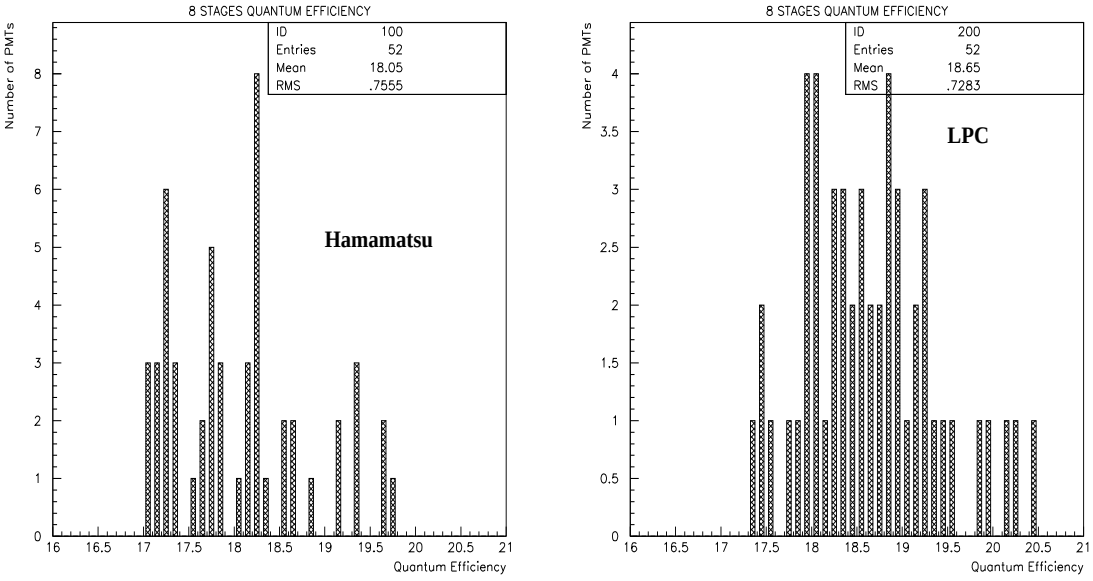

Figure 2: *Results of Quantum Efficiency by Hamamatsu and LPC.*

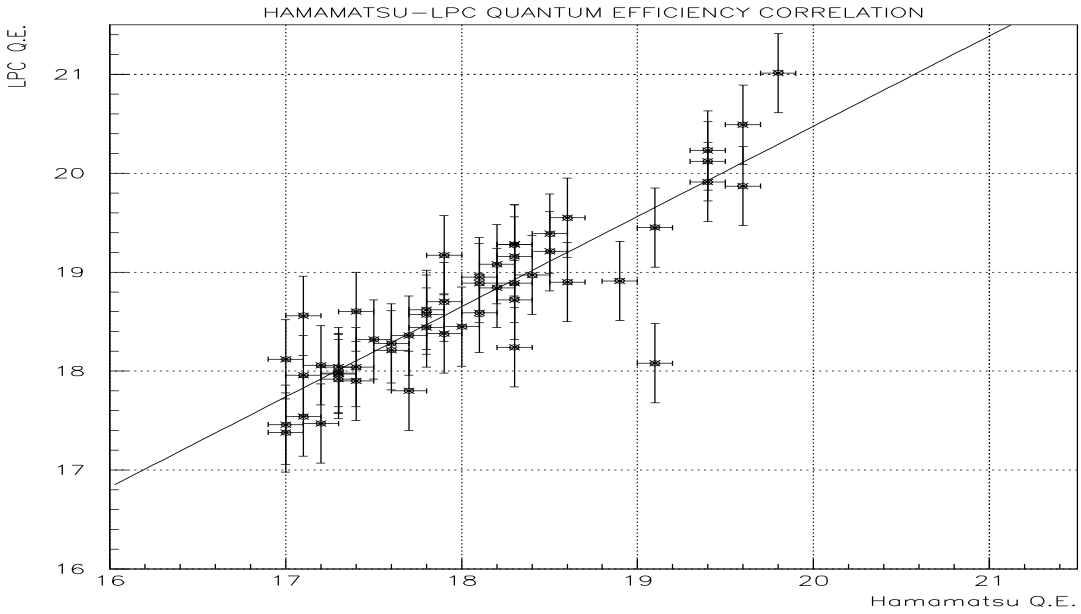

Figure 3: *Hamamatsu-LPC Quantum Efficiency Correlation.*

2. Relative Photocathode sensitivity

The measurement of the relative photocathode sensitivity was done for twenty PMTs only. We put the LED in DC mode and the special dividers in photocathode mode. We measured the current for each applied voltage between the photocathode and the first dynode, from 0 to 95 volts aproximately. Results are shown in figure 4.

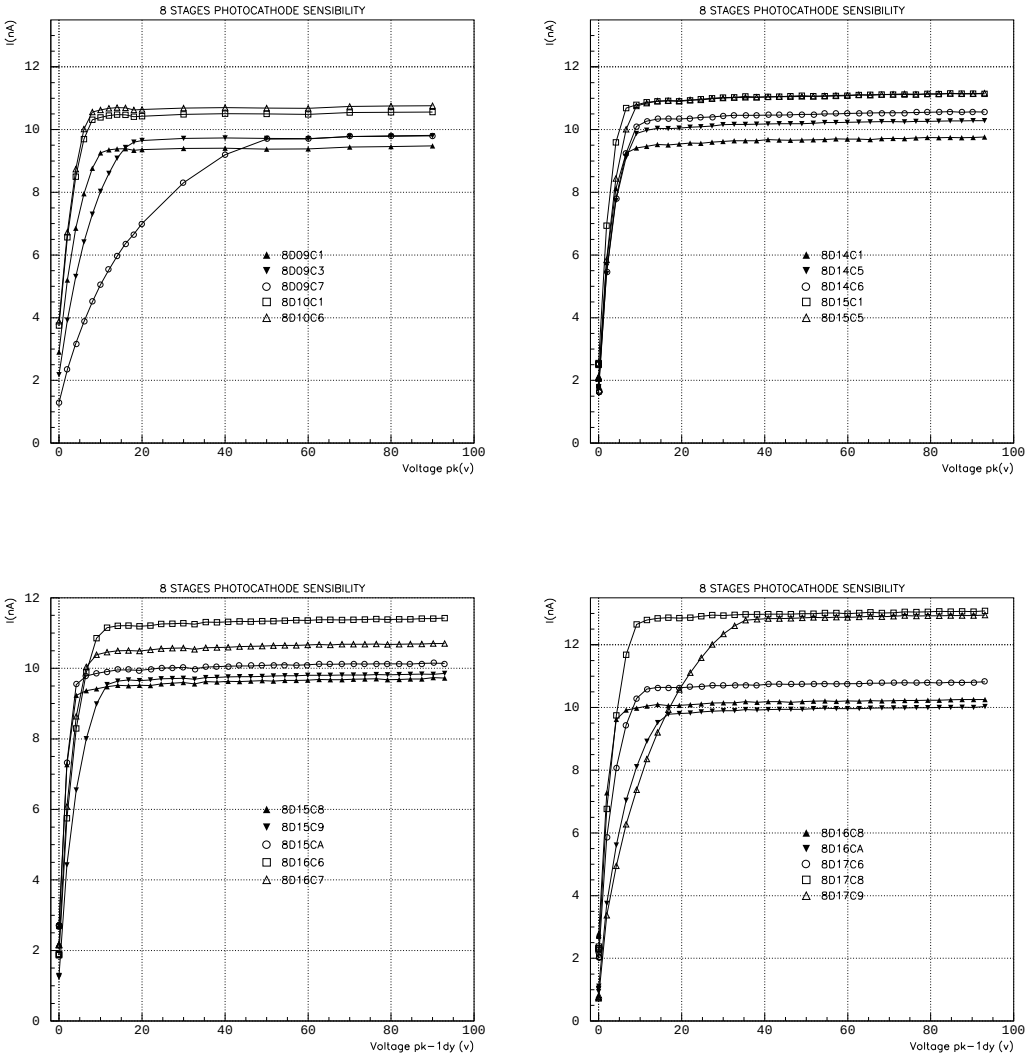

Figure 4: *Relative Photocathode Sensitivity.*

3. Current amplification in DC Mode

The PMTs are operated during the test beam at the nominal amplification of 10^5. That is why it is crucial to know what is the nominal voltage associated to this gain. It is also very important to know the variation of the gain with the high voltage for the intercalibration of the cells in the module (gain setting).

In order to measure the current amplification, we illuminate the photomultiplier with a DC light. Then we measure the anode current and photocathode current with the same light-flux. The gain of the photomultiplier is then given by:

$$Gain = \frac{I_{anode}}{I_{pk}} \tag{2}$$

where I_{anode} is the current measured in the normal operating condition and I_{pk} is the current measured without amplification.

These measurements are done using the special dividers, which allow to switch between the two operating modes: anode or photocathode mode. We did the measurements covering a range of ± 150 volts around the nominal voltage. The results are shown in figure 5 and the distribution of the nominal high voltage for a gain of 10^5 are plotted in figure 6.

Some PMTs present a down deviation at hight voltages respect to the behavior $lgG = lg\alpha + \beta lgV$, this is due to the saturation of the electronic with the big quantity of charge produced.

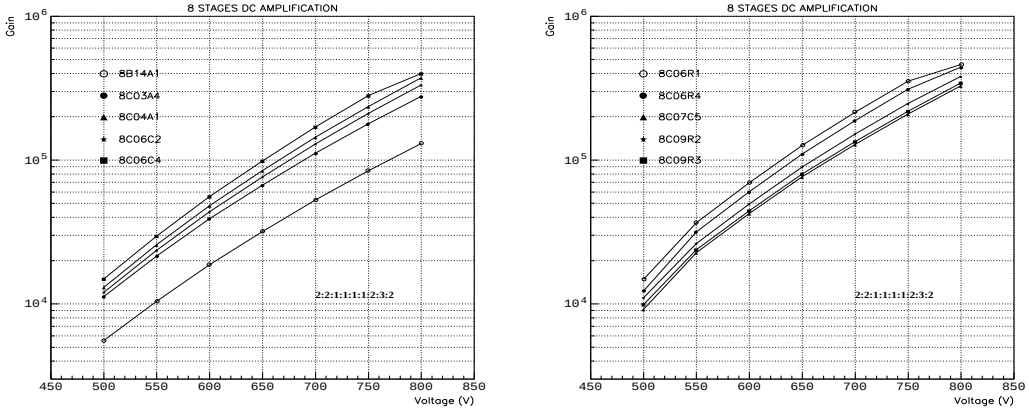

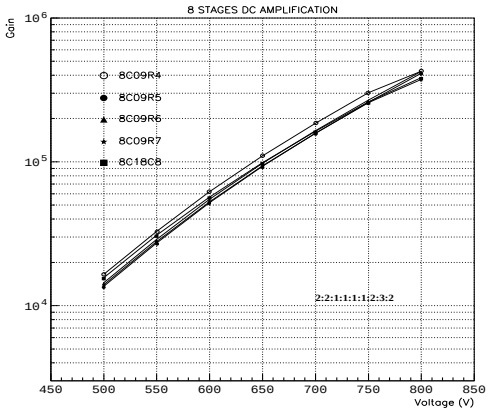
8 STAGES DC AMPLIFICATION
Gain
Voltage (V)
8C09R4
8C09R5
8C09R6
8C09R7
8C18C8
2:2:1:1:1:1:2:3:2

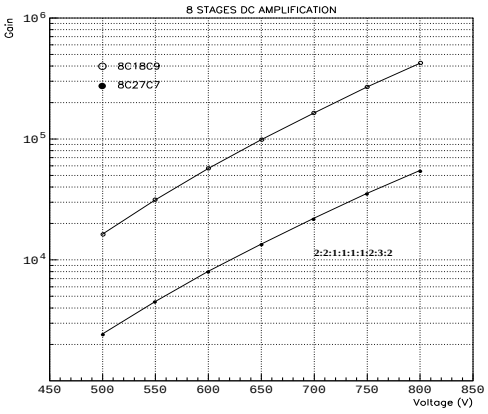
8 STAGES DC AMPLIFICATION
Gain
Voltage (V)
8C18C9
8C27C7
2:2:1:1:1:1:2:3:2

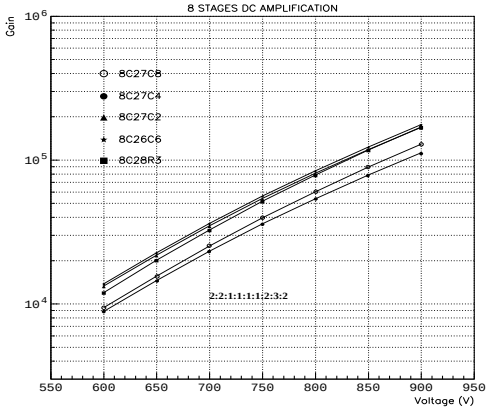
8 STAGES DC AMPLIFICATION
Gain
Voltage (V)
8C27C8
8C27C4
8C27C2
8C26C6
8C28R3
2:2:1:1:1:1:2:3:2

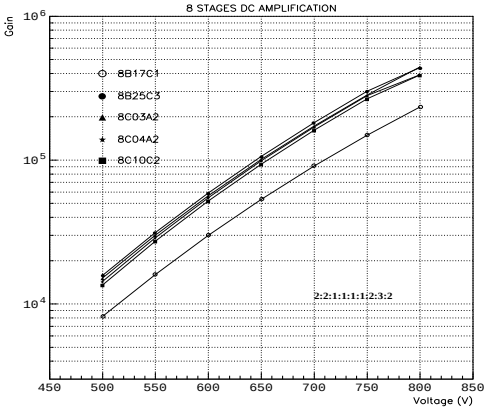
8 STAGES DC AMPLIFICATION
Gain
Voltage (V)
8B17C1
8B25C3
8C03A2
8C04A2
8C10C2
2:2:1:1:1:1:2:3:2

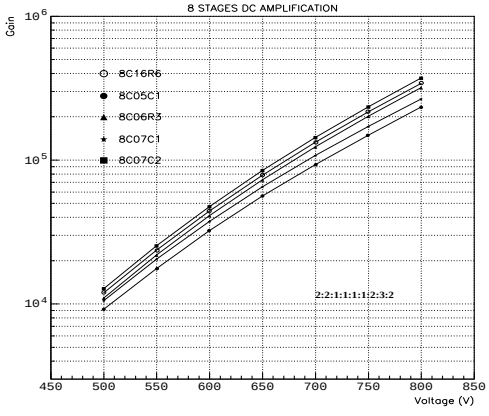
8 STAGES DC AMPLIFICATION
Gain
Voltage (V)
8C16R6
8C05C1
8C06R3
8C07C1
8C07C2
2:2:1:1:1:1:2:3:2

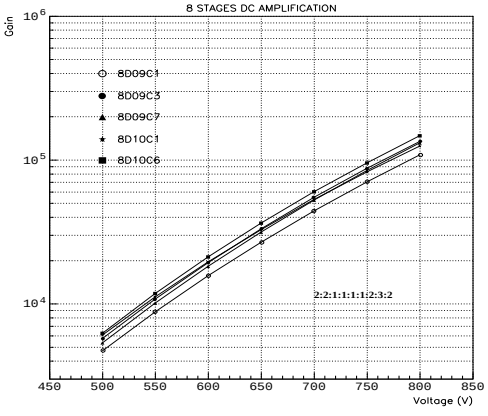
8 STAGES DC AMPLIFICATION
Gain
Voltage (V)
8D09C1
8D09C3
8D09C7
8D10C1
8D10C6
2:2:1:1:1:1:2:3:2

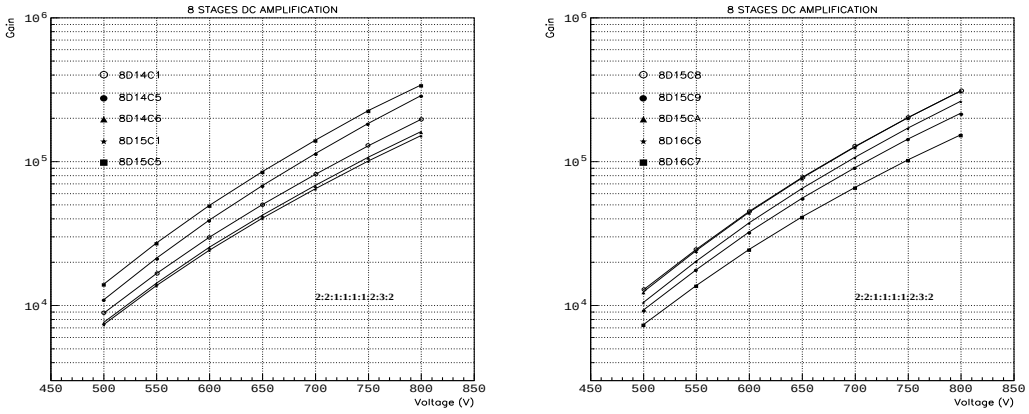

Figure 5: DC Amplification

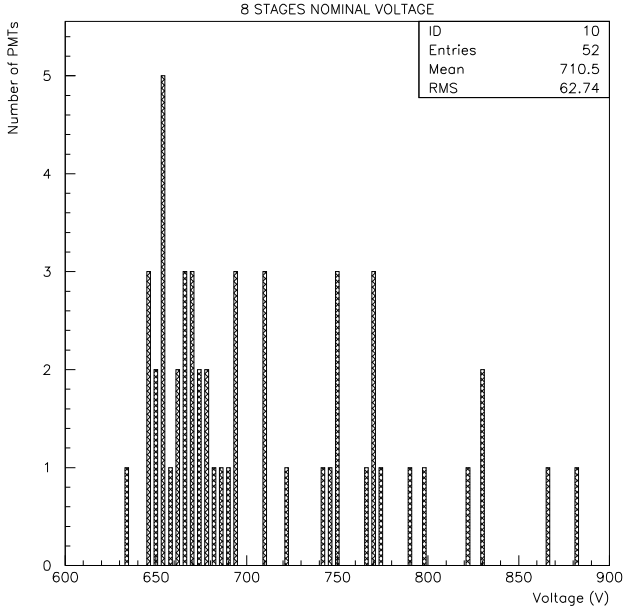

Figure 6: Nominal Voltage.

4. Amplification in Pulsed Mode

Amplication measurement in pulsed mode is based in the statistical result on the number of photoelectrons [4,5]:

$$N_{pe} = (\frac{\mu - \mu_{ped}}{\sigma})^2 \tag{3}$$

where μ represents the mean value of the distribution, μ_{ped} the pedestal, and σ the sigma of the distribution. Knowing the number of photoelectrons, the Gain (G) of the PMT is obtained from the PMT output charge in Coulomb Q:

$$N_{pe} \times G \times 1.6 \times 10^{-19} = Q \tag{4}$$

To perform PMT amplification in pulsed mode we associate to each PMT a standard divider. The LED was operated with 1kHz frequency and 20ns wide. The signals were measured by the use of a charge ADC.

There is a clear discrepancy between the values obtained in DC and in Pulsed mode. The *noise factor* correction, due to the statistical noise in the amplification procedure, can explain part of the differencies. Additional discrepancy could come from the DC mode procedure, where collection efficiency is ignored when measuring photocathode current. Figure 7 shows the distribution of amplification measured in pulsed mode and the same values, but corrected by the *noise factor*.

- **Noise factor correction.**

Assuming cascade events statistics in the dynode amplification in our PMTs we have the following expressions for the gain and fluctuation [3]:

$$\langle m_8 \rangle = \prod_{i=1}^{i=8} k_i \tag{5}$$

and

$$\sigma^2_{\langle m_8 \rangle} = (\langle m_8 \rangle)^2 \times [\frac{\sigma^2_{k1}}{k_1^2} + \frac{\sigma^2_{k2}}{k_1 k_2^2} + ... \frac{\sigma^2_{k8}}{(k_1 k_2 .... k_7 k_8^2}] \tag{6}$$

where k_i means the gain between dynodes i-1 and i, and σ_{ki} the variance. Defining F, the noise factor as:

$$F = [\frac{\sigma^2_{k1}}{k_1^2} + \frac{\sigma^2_{k2}}{k_1 k_2^2} + ... \frac{\sigma^2_{k8}}{k_1 k_2 .... k_7 k_8^2}] \tag{7}$$

and for the anode:

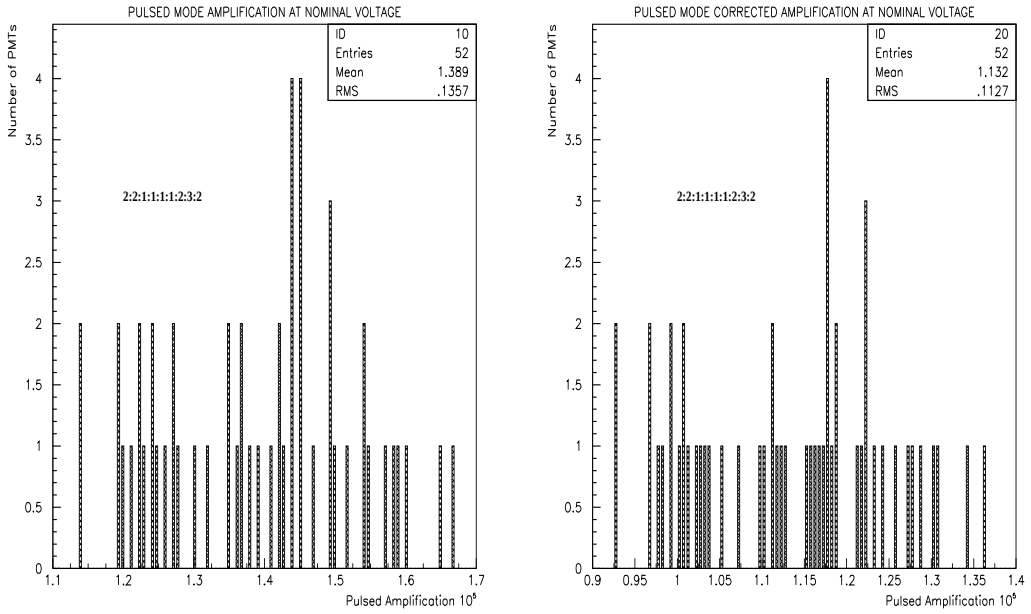

Figure 7: Pulsed Mode Amplification at Nominal Voltage and correction by the noise factor

$$N_a = N_{pk} \times k_1 \times k_2 \times ... \times k_8 \tag{8}$$

$$\sigma^2_{Na} = \langle m_8 \rangle^2 \sigma^2_{Npe} + N_{pe}\sigma^2_{\langle m8 \rangle} = \langle m_8 \rangle^2 \sigma^2_{N_\gamma} + N_\gamma \sigma^2_{m8} \tag{9}$$

After some straightforward calculations:

$$(\frac{N_a}{\sigma_{Na}})^2 = N_{pe} \times \frac{1}{1+F} \tag{10}$$

so, the noise factor corrected amplification is simply scaled by the factor 1/(1+F).

In this study we have used the 2:2:1:1:1:1:2:3:2 repartition, so the expresion (7) becomes:

$$F = \frac{1}{k_2}(1 + \frac{1}{k_2} - \frac{k_1}{k_2(1-k_1)}) \tag{11}$$

doing some trivial simplifications. Now the subindex i is refered to the value of the repartition. As we can see in expression 11, the noise factor depends slightly of the last values of the repartition, in particular the contribution of k_3 can be removed.

The values of k_1 and k_2 can be obtained from the nominal voltage, α and β results from the gain in DC measurements.

Example of PMT 8C06C14

From the gain measured in DC mode, the values of α, β and the nominal voltage are known ($G = \alpha V^{\beta}$).

$\alpha = 1.046E - 15$

$\beta = 7.1$

$V_{nominal} = 652$ volts

Taking in to account that the gain in one dynode is given by $k_1 = \alpha_1 v_1^{\beta_1}$, with $v_i = \frac{iV}{15}$ from the repartition, and the total gain can be expressed as $G = k_2^2 k_1^4 k_2 k_3$, the following values can be extracted :

$\alpha_1 = 0.117768$

$\beta_1 = 0.8875$

$k_1 = 3.3488$

$k_2 = 6.1952$

So finally the noise factor for this photomultiplier will be $F = 0.117768$.

5. Dark Current

The lower limit of light detection for a photomultiplier tube is determined by the electrical noise associated with the anode dark current. In TILECAL, the requirement for dark current is less than 1 nA at nominal voltage, and it has been supported for all the Hamamatsu generation of photomultipliers.

The dark current measurements are made after a warming up of more than one hour of the PMTs and the standard dividers. Results are presented in figure 8.

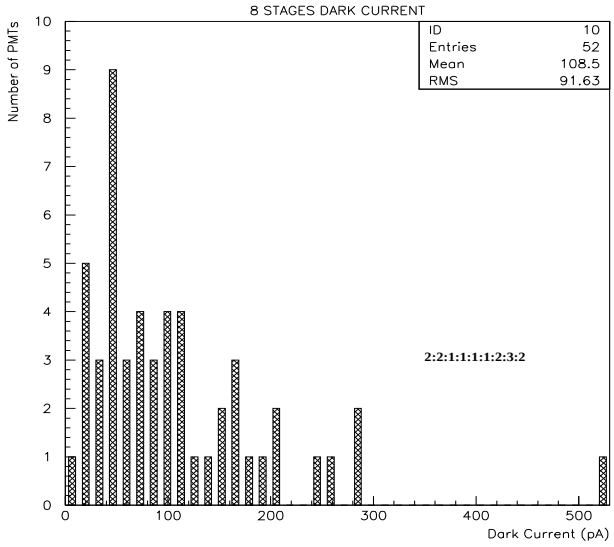

Figure 8: Dark Current.

6. Linearity

In ATLAS the PMTs must operate in a well-defined manner (linear) with light produced from small signals (muons) to high signals (large energy deposited in a single cell). The requirement is that the non-linearity of the tile calorimeter must be less than 2% for pulses of 15 ns and 50 mA of peak current in order to measure high energy jets with sufficient precision.

We did several measurements:

A) pulsed light at 1kHz (10 PMTs)

B) pulsed light at 1kHz plus 4 μA of DC light (5 PMTs)

C) pulsed light at 1kHz plus 2 μA of DC light (5 PMTs)

D) pulsed light at 100Hz (5 PMTs)

E) pulsed light at 100Hz plus 2 μA of DC light (5 PMTs)

The pulse width was 20ns. We used ten attenuation filters in order to get the different points, reaching an anode current up to 120mA. Figures 9, 10, 11, 12, 13, 14 show the linearity and deviation plots. The errors are due to the fit in points from 4 to 7 and to the calibration factors of the filters.

We can conclude from the study that the loss of linearity due to the superposition of DC light is not significative and the different frequencies of pulses have not effect on the linearity.

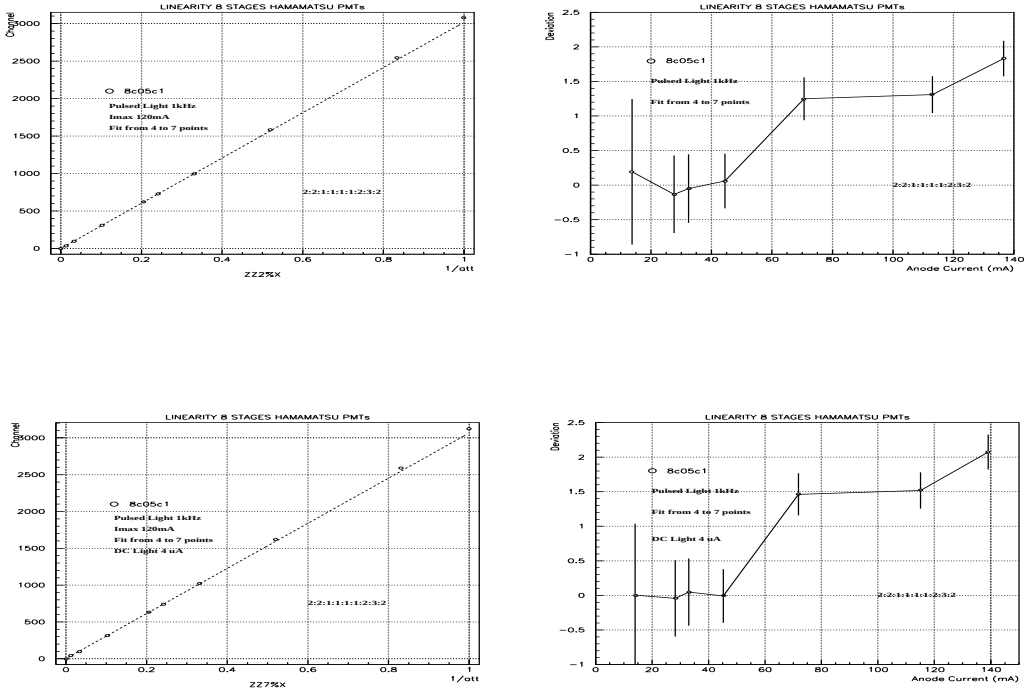

Figure 9: The largest deviation PMT. Section A,B

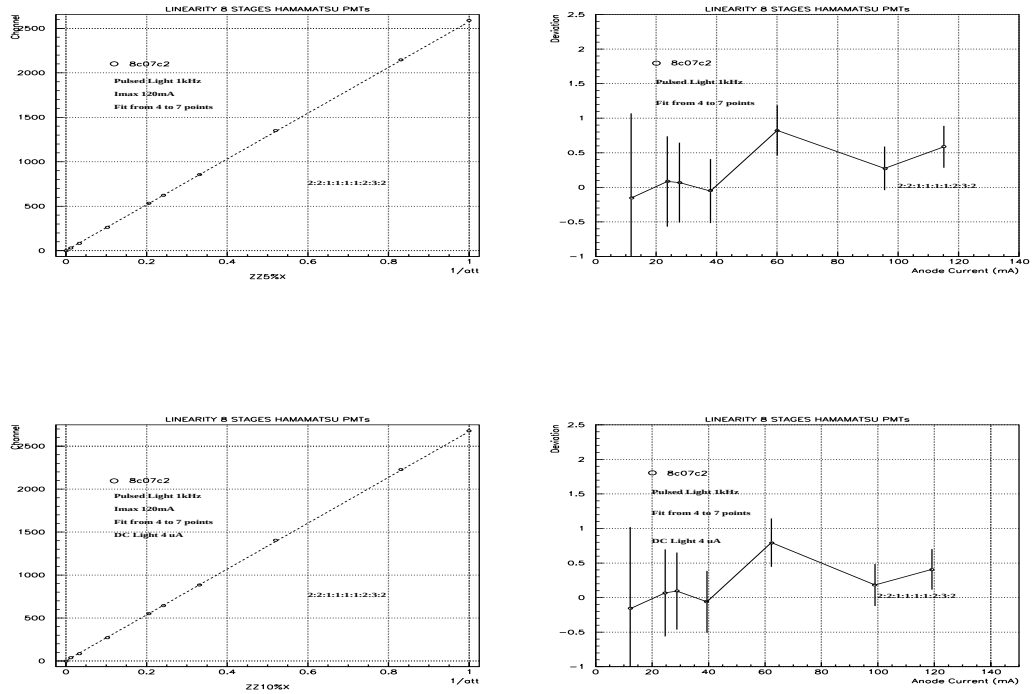

Figure 10: The smallest deviation PMT. Section A,B

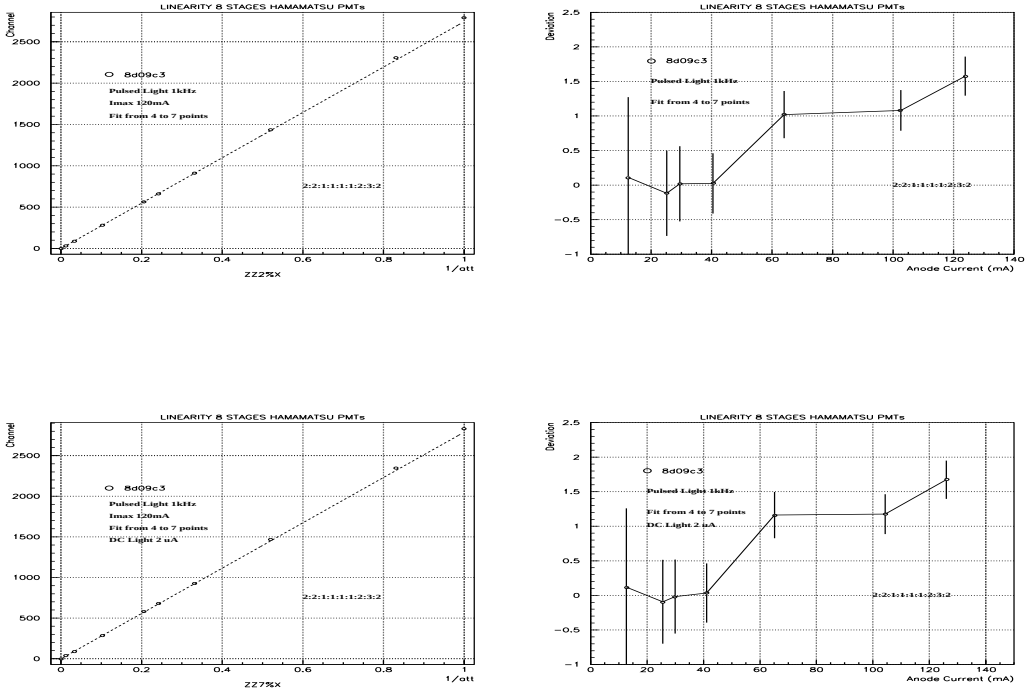

Figure 11: The largest deviation PMT. Section C

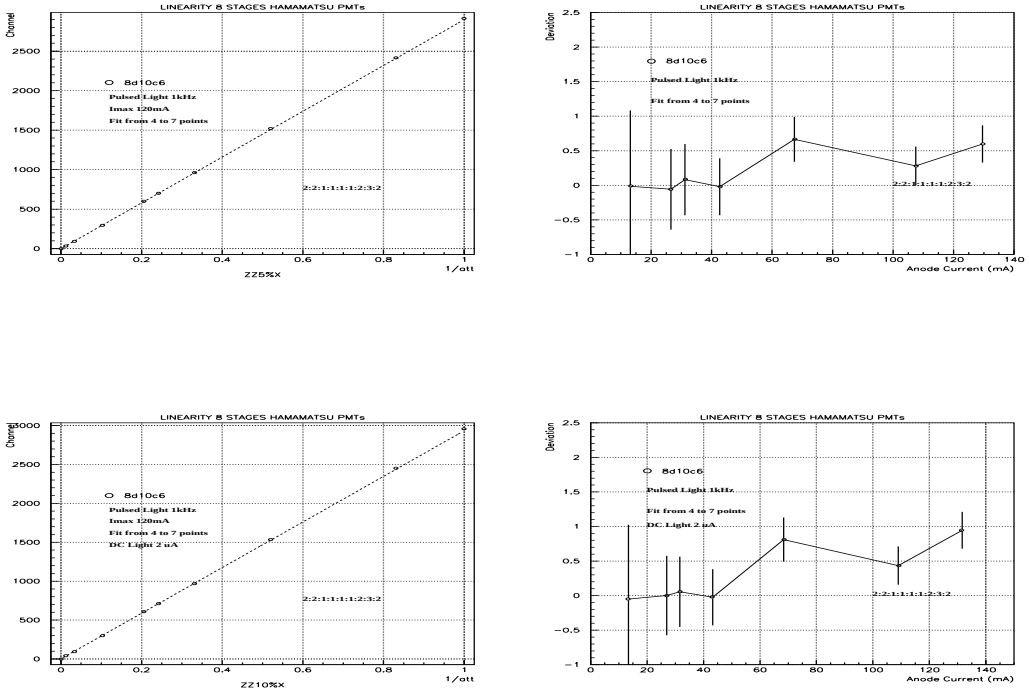

Figure 12: The smallest deviation PMT. Section C

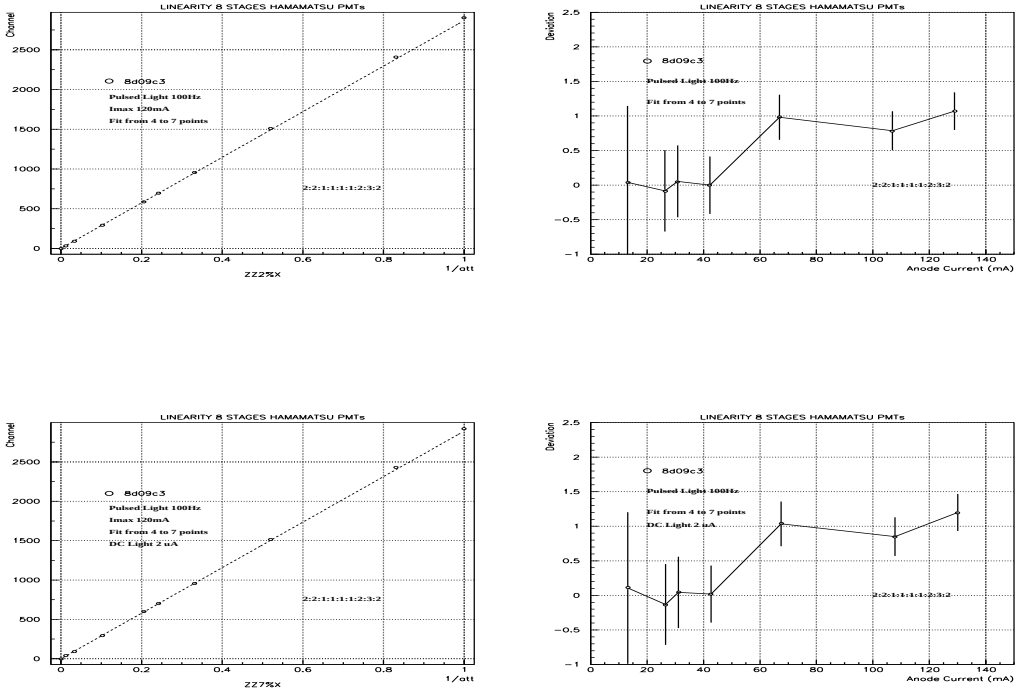

Figure 13: The largest deviation PMT. Section D,E

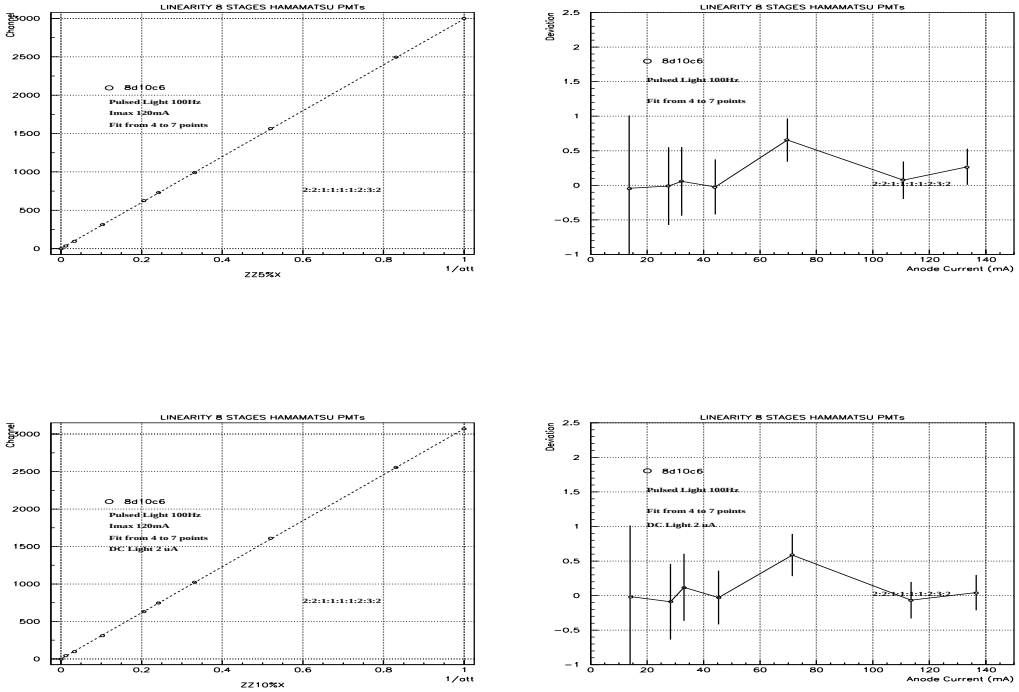

Figure 14: The smallest deviation PMT. Section D,E

7. Conclusions

For the last generation of R5900 8 stages Hamamatchu PMTs we can conclude from the measurements:

- There is a clear improvement in the quantum efficiency. From 16% to 18.5%.
- Good nominal voltage except for a few PMTs. Big dispersion, effect that will be very important for ten thousand PMTs.
- Pulsed gain not equal than gain in DC mode. Same behavior than before.
- Photocathode Sensitivity threshold above 10v.
- Dark current inside the requirements.
- Linearity inside the requirements $< 1\%$ for pulses of 20ns and 40mA currents. Loss of linearity up.

8. Summary of characteristics

We summarize here the results obtained on:

α and β for the expression $G = \alpha V^{\beta}$,

nominal voltage,

dark current,

pulsed gain,

the results from Hamamatsu,

and quantum efficiency.

Series number	α	β	HV_{nom} (v)	Dark Current (pA)	Pulsed Gain 10^5
8B14A1	4.083E-15	6.718	770	20	1.43
8C03A4	4.176E-15	6.828	690	110	1.58
8C04A1	7.081E-16	7.138	665	70	1.49
8C06C2	1.034E-15	7.064	670	100	1.65
8C06C4	1.046E-15	7.1	652	60	1.54
8C06R1	2.445E-17	7.715	632	20	1.42
8C06R4	5.270E-17	7.57	645	30	1.55
8C07C5	6.757E-17	7.478	675	30	1.45
8C09R2	9.385E-17	7.452	662	20	1.49
8C09R3	9.640E-17	7.431	671	30	1.49
8C09R4	2.053E-15	7.01	644	50	1.52
8C09R5	3.512E-16	7.259	658	20	1.59
8C09R6	5.561E-16	7.195	655	110	1.45
8C09R7	1.216E-15	7.066	660	40	1.45
8C18C8	5.556E-15	6.84	655	40	1.44
8C18C9	3.511E-15	6.915	650	70	1.5
8C26C6	3.296E-15	6.619	820	80	1.54
8C27C2	4.858E-15	6.625	828	110	1.45
8C27C4	3.275E-15	6.691	880	520	1.47
8C27C7	2.392E-15	6.767	797	290	1.37
8C27C8	9.959E-15	6.47	865	200	1.39
8C28R3	7.553E-15	6.551	830	140	1.37

Series number	α	β	HV_{nom} (v)	Dark Current (pA)	Pulsed Gain 10^5
8B17C1	4.000E-16	7.155	710	70	1.36
8B25C3	7.256E-16	7.167	645	60	1.44
8C03A2	5.405E-16	7.206	650	40	1.35
8C04A2	7.105E-16	7.157	652	100	1.42
8C10C2	4.178E-16	7.232	655	200	1.41
8C16R6	6.648E-16	7.135	675	50	1.44
8C05C1	2.370E-15	6.887	710	50	1.67
8C06R3	5.142E-16	7.163	680	150	1.6
8C07C1	3.187E-15	6.864	695	160	1.57
8C07C2	5.565E-16	7.174	665	190	1.44
8D09C1	4.16E-15	6.688	790	180	1.22
8D09C3	4.04E-15	6.725	765	160	1.14
8D09C7	2.03E-15	6.825	770	290	1.23
8D10C1	2.42E-14	6.447	772	100	1.21
8D10C6	4.23E-15	6.732	750	120	1.14
8D14C1	1.385E-14	6.598	721	40	1.28
8D14C5	1.915E-15	6.951	686	250	1.20
8D14C6	3.313E-14	6.493	742	100	1.27
8D15C1	3.259E-14	6.432	750	50	1.30
8D15C5	6.260E-15	6.802	664	70	1.26
8D15C8	6.415E-15	6.783	678	80	1.22
8D15C9	6.729E-15	6.723	711	260	1.19
8D15CA	4.061E-15	6.852	676	60	1.35
8D16C6	3.205E-15	6.862	694	170	1.24
8D16C7	2.49E-14	6.475	748	80	1.25
8D16C8	3.047E-15	6.871	692	20	1.24
8D16CA	6.541E-15	6.683	745	110	1.27
8D17C6	4.142E-15	6.719	769	150	1.38
8D17C8	6.505E-15	6.794	670	40	1.32
8D17C9	2.536E-15	6.855	720	340	1.19

Series Number	Cathode Luminous sens. (μA/lm)	Anode Luminous Sens. (A/lm)	Anode Dark Current (nA)	Cathode Blue Sens. (μA/lm)	Hamamatsu Quantum Efficiency (%)	LPC Quantum Efficiency (%)
8B14A1	89.6	9.3	0.08	10	18.9	18.91
8C03A4	89	27	0.98	10.2	17.6	18.21
8C04A1	96.3	32.2	0.83	9.58	17.9	18.38
8C06C2	89.5	27.7	4.24	9.47	17.1	17.54
8C06C4	90.4	34.4	3.05	8.84	17.7	17.8
8C06R1	91.4	43.6	7.31	8.95	17.3	17.92
8C06R4	91.9	38.4	3.3	9.17	17.8	18.62
8C07C5	84.6	28.1	0.67	9.96	17	18.12
8C09R2	86.2	36.1	0.32	9.74	17.8	18.57
8C09R3	94.1	29.6	0.17	10.2	18.1	18.59
8C09R4	90	34.4	0.92	10.1	19.1	19.45
8C09R5	90	31	0.14	9.72	18.2	19.08
8C09R6	82.6	31.1	0.13	10.4	18.1	18.89
8C09R7	90	31.8	0.14	10.7	19.1	18.08
8C18C8	92.8	40.8	3.41	9.61	18.2	18.84
8C18C9	90	41.1	0.66	9.71	18.3	19.28
8C26C6	96	7	0.22	9.32	17.3	18.04
8C27C2	87.7	8.1	0.9	9.3	17.2	18.06
8C27C4	88.6	5.1	0.58	9.45	17.4	18.04
8C27C7	86.9	9	0.19	9.49	17.2	17.47
8C27C8	90.1	5.7	1.65	9.78	17.3	17.98
8C28R3	91.9	6.8	0.73	9.41	17.8	18.44
8B17C1	92.8	19.7	0.05	10.2	19.4	20.12
8B25C3	86.5	36.6	0.12	9.27	17.1	18.56
8C03A2	80.3	27	0.09	9.67	17.3	17.97
8C04A2	85.5	32	0.45	9.37	17.1	17.96
8C10C2	93.5	30	1.48	9.67	17.6	18.28

Series Number	Cathode Luminous sens. (μA/lm)	Anode Luminous Sens. (A/lm)	Anode Dark Current (nA)	Cathode Blue Sens. (μA/lm)	Hamamatsu Quantum Efficiency (%)	LPC Quantum Efficiency (%)
8C16R6	83.5	24.9	0.74	9.59	17	17.38
8C05C1	89.6	21.5	0.27	9.35	17.5	18.32
8C06R3	94.1	28.3	4.23	9.69	17.7	18.36
8C07C1	92.4	25.5	0.94	9.61	18.3	18.72
8C07C2	79.7	20.3	0.59	9.46	17	17.46
8D09C1	99.4	12	0.17	10.2	19.4	19.91
8D09C3	99.9	14.9	1.61	10.2	19.4	20.23
8D09C7	86	12.9	0.51	9.51	18.6	19.55
8D10C1	92.5	12.4	0.09	9.67	18.5	19.39
8D10C6	101	14.9	0.98	10.3	19.6	19.87
8D14C1	92.1	18.6	0.06	9.29	18.0	18.48
8D14C5	100.0	25.6	0.56	9.75	17.9	19.17
8D14C6	101.0	13.3	0.16	9.55	18.3	19.28
8D15C1	95.2	15.9	0.07	9.60	18.3	18.24
8D15C5	97.9	30.0	0.35	9.60	18.3	18.89
8D15C8	100.0	32.4	0.31	9.43	18.4	18.97
8D15C9	99.8	20.1	0.53	9.43	18.1	18.95
8D15CA	101.0	35.3	0.44	9.69	18.3	19.16
8D16C6	105.0	22.2	0.19	10.30	18.5	19.21
8D16C7	94.7	16.2	0.31	9.72	17.9	18.70
8D16C8	91.4	26.8	0.04	9.69	17.4	18.60
8D16CA	92.0	13.9	0.08	9.83	17.4	17.90
8D17C6	101.0	12.6	0.28	10.50	18.6	18.89
8D17C8	105.0	32.9	1.14	11.00	19.6	20.49
8D17C9	109.0	23.1	0.67	11.10	19.8	21.01

Table 2: *Characteristics of the 52 PMTs for the Module 0*

9. References

[1] M.Crouau, et al. Technical characteristics of the prototype of the TILECAL photomultipliers test-bench. ATL-TILECAL-98-148. 23 Mar 1998.

[2] Atlas Collaboration, Tile Calorimeter Technical Design Report, CERN/LHCC/96-42, ATLAS TDR 3 (15 December 1996).

[3] G. Montarou, et al. Characterization of the Hamamatsu 10-stages R5900 photomultipliers at Clermont for the TILE calorimeter. 28 Apr.1997. TILECAL-NO-108.

[4] Burle Industries.Tube Products Division. Photomultiplier Handbook, 1980.

[5] S. Gonzalez de la Hoz. Estudio de la estabilidad de los parámetros de los fotomultiplicadores, en base a los requisitos establecidos para el Calorímetro Hadrónico TILECAL de ATLAS. Tesis de licenciatura. Diciembre de 1997.